MDPI

Article

Designing Dynamic Inductive Charging Infrastructures for Airport Aprons with Multiple Vehicle Types

Justine Broihan [1,2], Inka Nozinski [1,2], Niklas Pöch [1,2] and Stefan Helber [1,*]

1 Department of Production Management, Leibniz University Hannover, 30167 Hannover, Germany; justine.broihan@prod.uni-hannover.de (J.B.); inka.nozinski@prod.uni-hannover.de (I.N.); niklas.poech@prod.uni-hannover.de (N.P.)
2 Cluster of Excellence SE²A—Sustainable and Energy-Efficient Aviation, Technische Universität Braunschweig, 38106 Braunschweig, Germany
* Correspondence: stefan.helber@prod.uni-hannover.de; Tel.: +49-51-1762-5650

Abstract: In the effort to combat climate change, the CO_2 emissions of the aviation sector must be reduced. The traffic caused by numerous types of ground vehicles on airport aprons currently contributes to those emissions as the vehicles typically operate with combustion engines, which is why an electrification of those vehicles has already begun. While stationary conductive charging of the vehicles is the current standard technology, dynamic wireless charging might be an attractive technological alternative, in particular for airport aprons; however, designing a charging network for an airport apron is a challenging task with important technical and economic aspects. In this paper, we propose a model to characterize the problem, especially for cases of multiple types of vehicles sharing the same charging network, such as passenger buses and baggage vehicles. In a numerical study inspired by real-world airports, we design such charging networks subject to service level constraints and evaluate the resulting structures via a discrete-event simulation, and thus, show the way to assess the margin of safety with respect to the vehicle batteries' state of charge that is induced by the spatial structure of the charging network.

Keywords: dynamic wireless charging; electric vehicles; airport aprons

1. Introduction

A rising number of commercial airports across various countries declare their goal to implement carbon-neutral vehicle fleets as part of an overall reduction in CO_2 emissions in the aviation sector, which can be seen, for example, in [1–3]. An airport's vehicle fleet includes, for instance, baggage vehicles, passenger buses and catering vehicles [4]. Currently, many of these types of vehicle operating on the airport apron burn diesel fuel in combustion engines, and hence, contribute to the harmful CO_2 emissions. Several options are available for the electrification of the vehicle fleet such as battery swapping, conductive, static inductive and dynamic inductive recharging technologies. Battery-swapping technologies require a large number of identical batteries, as well as a battery replacement operation [5]. Conductive recharging leads to an increased downtime for vehicles during the charging process, and as a consequence, to an increased number of required vehicles. The same holds true for static inductive recharging technologies. One advantage of static inductive charging over conductive charging is that there is no need to plug the charging cable into the vehicle. Dynamic inductive recharging technologies, however, enable a vehicle to recharge while it is in motion [6]. The entire recharging of a vehicle, in principle, can be conducted during its service operations without any extra human intervention or charging-related downtime. Together with other advantages, which are discussed in Section 2, dynamic inductive charging might be a suitable charging technology for the numerous ground vehicles operating on airport aprons.

However, equipping an airport apron with a dynamic inductive charging infrastructure requires a structural arrangement of the various technical components. The two main investments in the infrastructure are Power Supply Units (PSUs), which provide an alternating current with the required frequency, and Inductive Transmitter Units (ITUs) placed below the road surface, which create an electromagnetic field used to transmit energy and to eventually charge the battery while a vehicle moves along an ITU. Since the installation of a dynamic inductive charging infrastructure involves major reconstruction work on the apron of an existing airport and requires long-term planning, it must be considered as a strategic planning problem. This is also supported by the fact that the expected utilization period of such an infrastructure is approximately 15 years [7]. These long-term decisions require a solid decision support methodology to which this paper aims to make a contribution.

Therefore, we study the problem to spatially locate the required dynamic inductive charging infrastructure components on the apron's road network to ensure that the required investment is as small as possible. First, we give a short overview of the components and characteristics of dynamic inductive charging infrastructures (Section 2.1) and airport aprons (Section 2.2). Section 2.3 contains a detailed description of the problem, followed by a discussion of related literature in the field of planning dynamic inductive charging infrastructures in Section 2.4. In Section 3.1, we develop a formal optimization model addressing the decision to spatially locate the charging infrastructure components in an economically efficient way. We introduce a reformulation of the mathematical formulation proposed in [8] and expand the problem definition by considering multiple differing vehicle types, as well as a service level constraint. In Section 3.2, we conduct a numerical study on several test instances, which are inspired by real-world airports. In this context, we have to consider the relationship between the design of the charging infrastructure and its impact on the State of Charge (SOC) of the vehicles' batteries as they operate on the apron.

The second goal of our study is to investigate the extent to which the design of the charging network facilitates a smooth operation of the electric vehicles with a sufficient SOC of their batteries. To study the fundamental aspects of this relationship, we perform a simplified discrete-event simulation of the transport operations on the apron in Section 4. In this simulation, the vehicle batteries are charged based on the strategically designed charging infrastructure determined by the mathematical model. This allows us to evaluate and validate the model results. Section 5 summarizes the findings of the paper.

2. Dynamic Inductive Charging on Airport Aprons

2.1. Dynamic Inductive Charging Infrastructures

Dynamic inductive charging is based on the technology of a wireless power transfer using electromagnetic fields [9]. Thus, primary coils (ITU in Figure 1) are embedded in the road asphalt or concrete and connected to the power grid. The secondary coil is installed underneath the electric vehicle (pick-up unit in Figure 1). As soon as the vehicle equipped with the pick-up unit travels along the ITUs, a magnetic field is generated, energy is transferred to the vehicle and its battery is charged. A PSU serves as a power supplier and generates an alternating current of the required frequency.
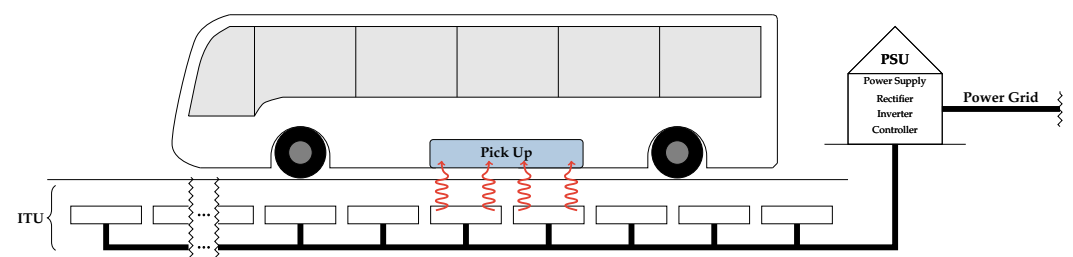

Figure 1. Components of the dynamic inductive charging system (Reprinted with permission from Helber et al. [8]).

The efficiency of the power transfer is highly dependent on the size of the air gap between the two coils [10,11]; however, studies show that an efficiency of around 95% can be achieved over air gaps of 100 mm to 175 mm [12–15]. Thus, this form of energy transfer appears to be appealing for flat surfaces and low-profiled vehicles, as they can be found on airport aprons. The initial investment in the charging infrastructure is costly, but it allows the use of smaller battery packs by around 20% [12]. In addition, a frequent recharging of the battery reduces charging downtimes [16] and increases the battery's lifespan [17].

Dynamic inductive charging systems are already implemented and tested in real-world applications. Examples include the well-known and intensively studied On-Line Electric Vehicle (OLEV) shuttling system at the Korea Advanced Institute of Science and Technology (KAIST) campus [6] and one of the first commercialized applications of dynamic inductive charging serving a public bus route in the city of Gumi in South Korea [18]. Additionally, there are more recent projects, such as the Smart Road Gotland [19] test track. A 1.6 km long dynamic inductive charging lane is embedded in a public street and wirelessly charges a 40 t long haul electric truck and an electric bus on the island of Gotland, Sweden [20,21]. Another recent project charges an urban electric shuttle bus on a 600 m long electric road in Tel Aviv, Israel [22].

2.2. Characteristics of Airport Apron Traffic

A typical commercial airport apron consists of aircraft parking positions that accommodate the aircraft during its turnaround process, aircraft service areas where the equipment loading and unloading takes place, as well as a road network for the apron vehicles [23]. Terminal buildings are adjacent to the airport apron, where gates and baggage sorting areas are located. In addition, vehicle depots are located in different areas of the airport apron and the buildings. An example of these apron components is shown in Figure 2.
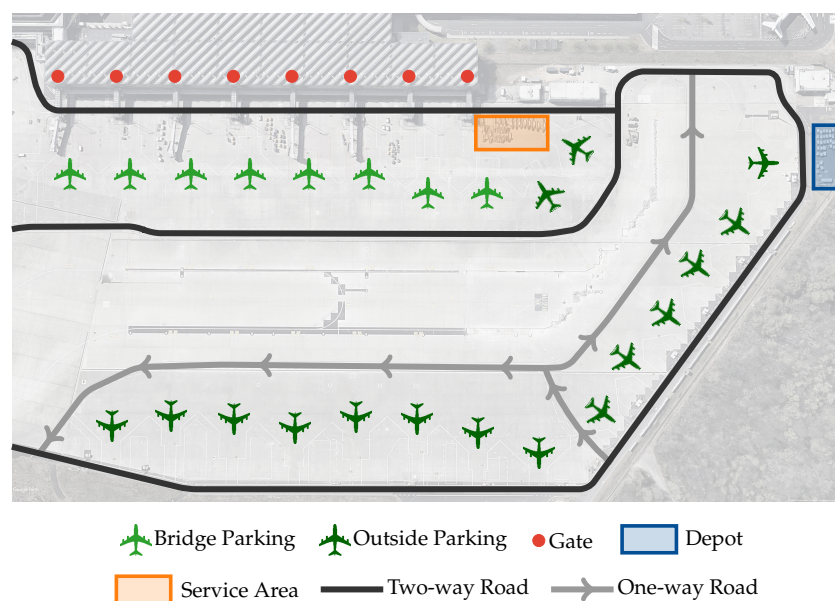
Figure 2. Selected part of the apron at Cologne Bonn Airport Source: Cologne Bonn Airport [online], 50°52′56″ N 7°07′10″ E, Height 574 m, Google Earth © GeoBasis-DE/BKG 2009, URL: http://www.google.com/earth on 29 June 2021.

An aircraft parks either at gate positions, where boarding takes place via passenger boarding bridges, or at outside parking positions. In the latter case, special passenger buses are typically used for the passenger transport between the terminal and the aircraft. The road system of the apron vehicles interconnects the individual gates, depots, service areas and parking positions. Most airports have a regular two-way road system with one

lane per direction, though one-way roads are possible. As in normal road traffic, specific road traffic rules, e.g., speed limits, apply.

Factors such as the size and type of the airport under consideration play a major role. While large hub airports handle many medium- and long-haul flights with high passenger volumes, smaller airports primarily handle medium- and short-haul flights with lower passenger volumes. In both cases, the smaller aircraft are often assigned to the less expensive outside parking positions to relieve terminal parking and reduce position costs at the expense of higher transportation cost for service personnel, baggage and passengers. (Position costs are charged by the airport depending on the duration of the turnaround process and the position on the apron. For additional information on airport operations and turnaround processes we refer to Schlegel [24], Ashford et al. [25] and Alonso Tabares and Mora-Camino [26].) Numerous vehicles of different types hence circulate on the road network on and beneath the airport apron in a very structured and foreseeable manner, which is essentially driven by the different processes required by the aircraft turnaround process. As parts of the apron road network are used by multiple different types of vehicles, the questions arise regarding to what extent they could share a common dynamic charging infrastructure if they were to be electrified.

2.3. Planning a Dynamic Inductive Charging Infrastructure for an Airport Apron

The location planning problem for an inductive charging infrastructure of an airport apron has to deal with two fundamental aspects of the problem.

- The first aspect stems from the need to enable a transfer of energy from the external power net, to which the airport is connected, to the electric vehicle being charged while in motion. As mentioned in Section 2, one major component is the PSU, that serves to invert the frequency and transform the voltage of the external power net to the required values for inductive charging. The second major component, the ITU, has to be connected (usually via neighboring ITUs) to a PSU in order to be operational. As the energy that can be transferred to a vehicle passing such an ITU-equipped road segment is substantially larger than the energy required to actually move that vehicle over the ITU-equipped road segment, it follows that only a relatively small part of the road network may have to be equipped with ITUs. This typically results in multiple installed PSUs and connected ITUs in different parts of the road network.

- The second aspect stems from the vehicles which, while moving on the apron, are always serving some request. An example of such a request could be for a passenger bus to drive from a bus depot to a particular aircraft parking position, pick up passengers and bring them to a specific gate. While serving such a request, the vehicle would follow a certain route. Along this route, a sufficient portion of the road network has to be equipped with ITUs to ensure that the vehicle can pick up at least as much energy as it requires to serve this request. If this condition holds true, then a sufficiently large battery of that vehicle would never be empty and the vehicle would never break down.

Thus, we have, on the one hand, the connection between the set of requests and their respective routing, and on the other hand, the aspect of ITUs and PSUs location. The overall objective of the location problem is to minimize the required investment in installed PSUs and ITUs.

An example of a fictitious placement of the components of a dynamic inductive charging infrastructure is depicted in Figure 3. The charging infrastructure consists of two independent charging tracks. One of the charging tracks allows vehicles moving along the terminal building to charge while they are in motion. The other charging track supplies vehicles in the depot area and on the outer right apron road when serving aircraft parked at outside parking positions. The respective PSUs are located at one of the gates at the terminal building and at the depot.

Figure 3. Exemplary dynamic inductive charging infrastructure on the apron of Cologne Bonn Airport. Source: Cologne Bonn Airport [online], 50°52′56″ N 7°07′10″ E, Height 574 m, Google Earth © GeoBasis-DE/BKG 2009, URL: http://www.google.com/earth on 29 June 2021.

It should be noted that we are dealing with strategical design questions, and the number of conceivable requests can be extremely large. Many of those requests, however, would be very similar in their routing, energy requirements, etc. In this situation it seems reasonable to work with a large but still controllable collection of representative requests, especially when we are dealing with multiple vehicle types, as well. We assume that both the considered ITU and PSU components are sufficiently powerful to deal with typical operational conditions of multiple moving vehicles being charged simultaneously.

In this situation, we want to avoid an overly conservative design where many more ITUs are installed than are actually needed. Thus, we will enable a certain fraction of the energy demands of requests to *not* be entirely met while serving the current request. Under typical operating conditions, this may still be feasible if, while serving the *next* request, the affected vehicle may have the opportunity to pick up more energy than required for that second request, and hence, eliminate its energy deficit stemming from the previous request. In order to study the effect of this "allowed energy deficit" in the system design from the first part of our study, we report on simulation results for those designs in the second part of our study.

2.4. Related Literature and Research Questions

Contributions to the field of the optimal placement of wireless charging components are provided in comprehensive reviews by Jang [27], Yatnalkar and Narman [28] and Majhi et al. [29]. Ushijima-Mwesigwa et al. [30] introduced an Integer Program (IP) formulation for the optimal placement of wireless charging lanes in public road networks for private vehicles considering a minimum investment objective. Liu et al. [31] and Khalaf et al. [32] studied an investment minimal placement of wireless charging lanes and optimal battery capacities for Binghamton University buses. Bi et al. [33] extended the minimum investment objective in their formulation using a multi-objective framework considering life cycle greenhouse gas emissions and energy consumption with regard to the lifetime of a wireless bus charging system. They present their findings based on the example of the bus routes of the University of Michigan. Hwang et al. [18] propose an Mixed Integer Program (MIP) that allocates the charging infrastructure in the context of multiple-route environments, where independent bus routes share common road segments. Considering the OLEV shuttling system developed at KAIST, Lee et al. [34] studied a Markov decision process-based optimization algorithm using reinforcement learning to estimate optimal battery capacities, pickup capacity and the number of ITUs. Mohamed et al. [35] focused their

work on the integration of a wireless charging system with automated driving. Iliopoulou and Kepaptsoglou [36] design a bi-level optimization related to a transit route network design and a charging infrastructure location problem in public transport. He et al. [37] proposed a Nonlinear Program (NLP) to deploy wireless charging lanes in public road traffic with regard to road capacities and route choices for travelers.

Except for Helber et al. [8], we are not aware of any work considering dynamic inductive charging systems on airport aprons. In this paper, we introduce a much more transparent and intuitive reformulation of the initial mathematical optimization model in Helber et al. [8] and expand the problem definition to a multiple vehicle approach with a service level restriction. In contrast to Helber et al. [8], we also conduct a numerical study using several real-sized test instances. Based on the resulting infrastructure obtained from the optimization process, we further investigate the validity of this strategically planned infrastructure in operational use via a discrete-event simulation. Thus, we address the following research questions within the scope of this paper:

- How can a dynamic inductive charging infrastructure for airport aprons with minimal investment be determined considering different types of vehicles?
- How can the validity of the assumptions and abstractions of the mathematical model for determining a dynamically inductive charging infrastructure be investigated and evaluated?

3. Modeling Dynamic Inductive Charging Infrastructures Considering Multiple Vehicle Types

3.1. Mathematical Model

To define our model formulation of the infrastructure design problem introduced in Section 2.3, we present the following assumptions and abstractions closely related to those in Helber et al. [8]. The underlying notation is introduced in Table 1.

- We model the road system of the airport apron as a directed and weighted planar connected digraph $G(\mathcal{V}, \mathcal{L})$ as pictured in Figure 4, which is composed of a set of vertices $v \in \mathcal{V}$ and a set of directed edges or links $l \in \mathcal{L}$.
- A vertex $v \in \mathcal{V}$ defines a particular geographic location on the airport apron. These include either gate positions (i.e., $g15$ in Figure 4), aircraft parking positions (i.e., $p18$ in Figure 4), depots (i.e., $d2$ in Figure 4), service areas (i.e., $bh1$ in Figure 4) or fixed positions in the road system to split road sections (i.e., $i21$ in Figure 4).
- Among the set of vertices $\mathcal{V}$, we define a subset $\mathcal{P} \subseteq \mathcal{V}$, which denotes the set of vertices $v \in \mathcal{V}$ qualified to host a PSU. The installation of a PSU at a candidate vertex $v \in \mathcal{P}$ requires to a fixed investment defined as $c_v^{psu} \in \mathbb{R}^{\geq 0}$.
- Every section of the airport apron's road system is defined as a directed link $l \in \mathcal{L}$ and connects a pair of distinct vertices $v \in \mathcal{V}$. The direction of each link $l \in \mathcal{L}$ denotes the direction of travel.
- Every link $l \in \mathcal{L}$ is a candidate to host an ITU. To supply such an ITU with electricity, it must be connected to a PSU. We define a set of links $\mathcal{L}_v \subset \mathcal{L}$, which are qualified to receive power from a PSU candidate at vertex $v \in \mathcal{P}$.
- The counterpart to $\mathcal{L}_v \subset \mathcal{L}$ is $\mathcal{P}_l \subseteq \mathcal{V}$. For each link $l \in \mathcal{L}$, $\mathcal{P}_l \subseteq \mathcal{V}$ contains a set of vertices that are suitable as PSU candidates.
- To ensure a connection from each ITUs to a PSU, we define a set of links $l' \in \Gamma_{lv} \subset \mathcal{L}$ for each combination of link l and PSU candidate v as $\Gamma_{lv} = \{l' \in \mathcal{L}_v \,|\, l'$ precedes l on shortest path to $v \in \mathcal{PSU}\}$.
- $\mathcal{LP}_v \subset \mathcal{L}$ defines a set of links l directly neighboring a PSU candidate $v \in \mathcal{P}$.
- The installation of an ITU at link $l \in \mathcal{L}$ requires a fixed investment denoted by $c_l^{itu} \in \mathbb{R}^{\geq 0}$.
- A vehicle type $t \in \mathcal{T}$ defines a particular class of service vehicles. Each vehicle type is assigned to specific service tasks in the turnaround process of an aircraft, i.e., passenger and baggage transfers, catering and cleaning.

- We define service requests $r \in \mathcal{R}$ that represent the apron vehicles' potential service tasks, e.g., passenger transfers from a gate to an aircraft or baggage transportation.
- Among the set of service requests $r \in \mathcal{R}$, we define a subset $\mathcal{R}_t \subseteq \mathcal{R}$, which assigns service requests $r \in \mathcal{R}$ to the corresponding vehicle type $t \in \mathcal{T}$. For example, a baggage tractor never approaches a gate and a passenger bus never approaches the baggage handling area. Accordingly, $\mathcal{R}_{\text{Bus}}$ does not contain any requests that lead to the baggage handling area, except for those that serve to transport passengers.
- Every request $r \in \mathcal{R}$ is composed of a set of links $l \in \mathcal{L}_r$, which must be traveled to satisfy that particular request.
- Traveling on a link $l \in \mathcal{L}$, which is equipped with an ITU, allows the vehicle a fixed amount of energy intake $ei_{lt} \in \mathbb{R}^{\geq 0}$, depending on the vehicle type $t \in \mathcal{T}$, which in turn enables the vehicle to charge its battery.
- The consumed energy for a particular request $r \in \mathcal{R}$ by traveling along the links in $\mathcal{L}_r \subseteq \mathcal{L}$ with a corresponding vehicle of type $t \in \mathcal{T}$ is denoted by $ec_{rt} \in \mathbb{R}^{\geq 0}$.
- An overall fraction β of the energy required over the different types of vehicles and their respective service requests has to be met by the installed ITU infrastructure.

Table 1. Notation used in the dic-mv model.

| Indices and Sets	
$v \in \mathcal{V}$	vertices $\mathcal{V} := \{1, \dots, V\}$
$l \in \mathcal{L}$	links $\mathcal{L} := \{1, \dots, L\}$
$r \in \mathcal{R}$	service requests $\mathcal{R} := \{1, \dots, R\}$
$t \in \mathcal{T}$	vehicle types $\mathcal{T} := \{1, \dots, T\}$
$\mathcal{P} \subseteq \mathcal{V}$	set of vertices $v \in \mathcal{V}$ qualified to host a PSU
$\mathcal{P}_l \subseteq \mathcal{V}$	set of PSU candidates able to supply link $l \in \mathcal{L}$
$\mathcal{L}_v \subset \mathcal{L}$	set of links $l \in \mathcal{L}$ qualified to be powered by a PSU candidate at $v \in \mathcal{P}$
$\mathcal{L}_r \subseteq \mathcal{L}$	set of links $l \in \mathcal{L}$ included in service request $r \in \mathcal{R}$
$\mathcal{R}_t \subseteq \mathcal{R}$	set of requests $r \in \mathcal{R}$ serviced by vehicle type $t \in \mathcal{T}$
$\mathcal{LP}_v \subset \mathcal{L}$	set of links $l \in \mathcal{L}$ directly neighboring a PSU candidate at $v \in \mathcal{P}$
$\Gamma_{lv} \subset \mathcal{L}$	set of predecessors $l' \in \mathcal{L}$ of link $l \in \mathcal{L}$ in a direct connection on the shortest path to a PSU candidate at $v \in \mathcal{P}$
Parameters	
$\beta \in [0, 1]$	service level parameter
$c_v^{psu} \in \mathbb{R}^{\geq 0}$	investment in a PSU at vertex $v \in \mathcal{P}$
$c_l^{itu} \in \mathbb{R}^{\geq 0}$	investment in an ITU at link $l \in \mathcal{L}$
$ei_{lt} \in \mathbb{R}^{\geq 0}$	energy intake by traveling along link $l \in \mathcal{L}$ with vehicle type $t \in \mathcal{T}$
$ec_{rt} \in \mathbb{R}^{\geq 0}$	energy consumption by serving request $r \in \mathcal{R}$ with vehicle type $t \in \mathcal{T}$
Decision Variables	
$E_{rt} \in \mathbb{R}^{\geq 0}$	amount of energy consumption that is not satisfied for service request $r \in \mathcal{R}$ and vehicle type $t \in \mathcal{T}$ (energy deficit)
$X_{lv} \in \{0, 1\}$	1, if link $l \in \mathcal{L}$ is equipped with an ITU and powered by PSU at vertex $v \in \mathcal{P}$, 0 else
$Y_v \in \{0, 1\}$	1, if a PSU is installed at vertex $v \in \mathcal{P}$, 0 else
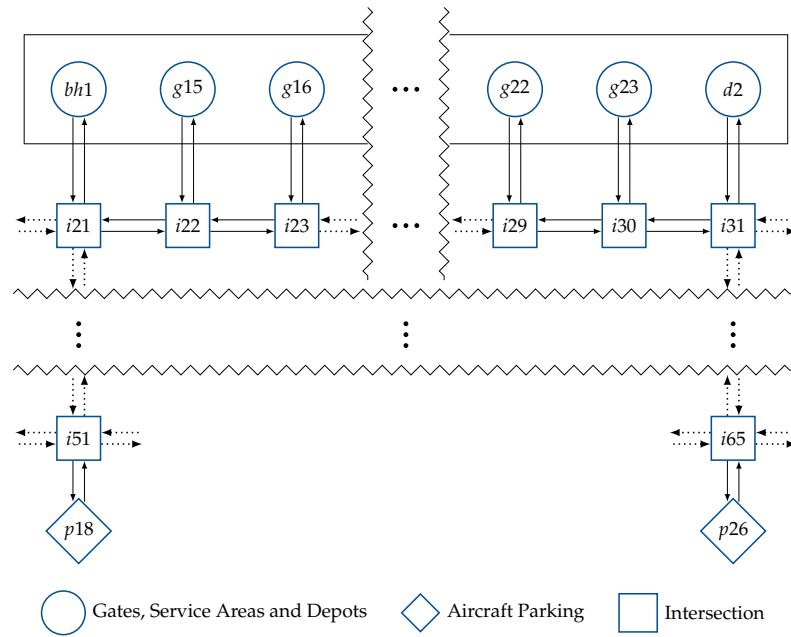
Figure 4. Representation of an airport as a planar digraph.

To describe a spatial distribution of the charging infrastructure, we introduce two binary and one continuous decision variables. Variable $Y_v \in \{0,1\}$ takes a value of 1 if a PSU is installed at node $v \in \mathcal{P}$ and 0 otherwise. Likewise, $X_{lv} \in \{0,1\}$ takes a value of 1 if an ITU is installed at link $l \in \mathcal{L}_v$ and connected to a PSU at vertex $v \in \mathcal{P}$ and 0 otherwise. $E_{rt} \in \mathbb{R}^{\geq 0}$ describes the energy deficit of vehicle type $t \in \mathcal{T}$ serving request type $r \in \mathcal{R}_t$.

Based on the previous assumptions, we introduce the Dynamic Inductive Charging Problem considering Multiple Vehicle Types (DICP-MV) as an MIP as follows:

$$\min F = \sum_{v \in \mathcal{P}} \left(c_v^{psu} \cdot Y_v + \sum_{l \in \mathcal{L}_v} c_l^{itu} \cdot X_{lv} \right) \tag{1}$$

s.t.

$$\sum_{v \in \mathcal{P}} \sum_{l \in \mathcal{L}_r \cap \mathcal{L}_v} X_{lv} \cdot ei_{lt} \geq ec_{rt} - E_{rt} \qquad t \in \mathcal{T}, r \in \mathcal{R}_t \tag{2}$$

$$\sum_{t \in \mathcal{T}} \sum_{r \in \mathcal{R}_t} E_{rt} \leq (1 - \beta) \cdot \sum_{t \in \mathcal{T}} \sum_{r \in \mathcal{R}_t} ec_{rt} \tag{3}$$

$$X_{lv} \leq Y_v \qquad v \in \mathcal{P}, l \in \mathcal{L}_v \tag{4}$$

$$\sum_{v \in \mathcal{P}_l} X_{lv} \leq 1 \qquad l \in \mathcal{L} \tag{5}$$

$$\sum_{l' \in \Gamma_{lv}} X_{l'v} \geq X_{lv} \qquad v \in \mathcal{P}, l \in \mathcal{L}_v \setminus \mathcal{LP}_v \tag{6}$$

$$X_{lv}, Y_v \in \{0,1\} \qquad v \in \mathcal{P}, l \in \mathcal{L}_v \tag{7}$$

$$E_{rt} \in \mathbb{R}^{\geq 0} \qquad t \in \mathcal{T}, r \in \mathcal{R}_t \tag{8}$$

In the objective function (1), we minimize the total investment in dynamic inductive charging infrastructure components. Constraint (2) determines the possible energy deficit

for each vehicle type $t \in \mathcal{T}$ on service request $r \in \mathcal{R}_t$. Constraint (3) poses an aggregate upper bound on the energy deficits. In Restriction (4) we state that an ITU can only be connected to an installed PSU. Each link $l \in \mathcal{L}$ can be equipped with at most one ITU and connected to at most one PSU, as seen in Constraint (5). Restriction (6) enforces a consistent and through-connected ITU infrastructure from the furthest ITU along a shortest path to the serving PSU.

3.2. Numerical Study

3.2.1. Description of Test Instances

We implemented the model introduced in Section 3.1 in Python 3.8 and solve instances of different sizes with the solver Gurobi 9.1.0. The computations were conducted on a single core of an Intel(R) IvyBridge Xeon E5-4650 v2 (10-core, 2.40 GHz, 25 MB Cache, 95 W). (The results were achieved by computations carried out on the cluster system at the Leibniz University Hannover, Germany.) We consider apron buses and baggage cars as vehicle types in all instances. A small fictitious network, closely related to the test instance in Helber et al. [8], is depicted in Figure 5. In the following, we refer to this network with five gates $g1$–$g5$ as the Fictitious Airport instance, to differentiate it from other instances inspired by real airports in the German cities of Stuttgart, Cologne and Hamburg. Both vehicle types can be parked at the depot $d1$. A baggage handling area is located at node $bh1$. We refer to the gates, the depot and the baggage handling area together as terminal nodes.
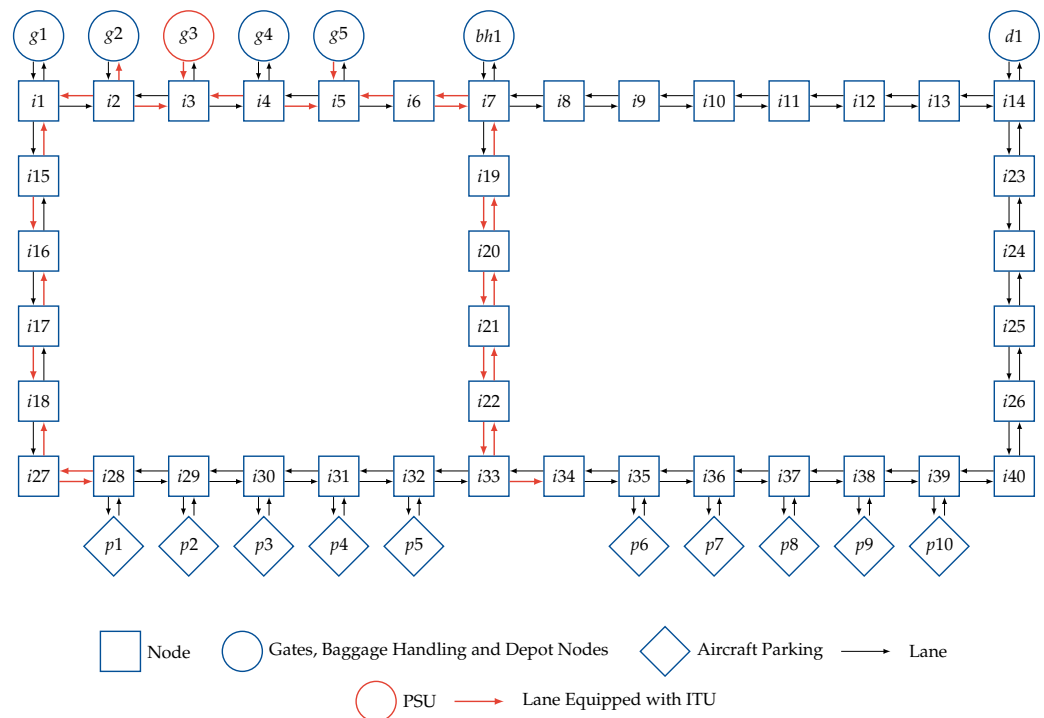
Figure 5. Graph of the Fictitious Airport instance (Note: Optimal charging infrastructure obtained with DICP-MV model.) Adapted with permission from Helber et al. [8].

We consider a two-way request structure for the service requests as described in Helber et al. [8]. Vehicles start at a terminal node, stop at an aircraft parking node and return to one of the terminal nodes. Each vehicle type approaches specific terminal nodes, i.e., buses start and end their trips at one of the gates or the depot, while baggage cars start and end their trips at the baggage handling area or at the depot. We consider each possible two-way request, except those requests where both the start and the end node are the depot. Consequently, the sets $\mathcal{R}_{\text{bus}}$ and $\mathcal{R}_{\text{baggage}}$ are mutually exclusive. In total, we consider 380 possible two-way requests in the Fictitious Airport instance. We assume that these requests are used most frequently; therefore, we do not consider additional requests

in our instance, e.g., we do not consider a single-way service request between two aircraft parking positions.

The Fictitious Airport instance consists of 57 nodes and 116 links. We assume that the link length varies between 25 m and 50 m. We assume that all links $l \in \mathcal{L}$ of the network can be equipped with an ITU and be powered by each possible PSU. PSUs requires a connection to the local power grid and can therefore only be installed at the terminal nodes.

The considered parameter values of our numerical study are shown in Table 2. We assume an ITU investment of 500 \$/m and a PSU investment of 50,000\$ per PSU based on Jeong et al. [17]. The energy consumption of a vehicle correlates to its size, weight and average velocity. For a typical electric apron bus, we refer to Siemens [38]. We assume that both vehicle types have identical pickup systems. Due to different speed limits, the vehicle types have different average energy intakes. Baggage cars are assumed to operate at a lower average speed of 20 km/h due to their trailer [39,40]. Consequently, they have a higher energy intake per meter traveled as they spent more time on the ITU. We assume a power of 100 kW and an efficiency of 80 % for the computation of the energy intake of the vehicle pick-up unit. If not mentioned otherwise, all calculations are performed with a value of $\beta = 1$, hence demanding that no request ever leads to an energy deficit.

Table 2. Parameter values for test instances.

ITU investment		500 \$/m
PSU investment		50,000 \$/unit
energy intake		
	bus	3.6 kWh/km
	baggage car	4.5 kWh/km
energy consumption		
	bus	1.11 kWh/km
	baggage car	0.54 kWh/km

In addition to the Fictitious Airport instance, we introduce three larger instances, inspired by the airports of Stuttgart (STR), Cologne (CGN) and Hamburg (HAM) in Germany. The spatial features of our models of those airports are deduced from satellite images of those airports and transformed into graphs of a nature such as that for the Fictitious Airport in Figure 5. Since we do not have detailed information on the exact structure, e.g., about specific roadway lengths or the position of depots, we place intermediate nodes $i1, i2, \ldots$ only at intersections, i.e., where a road branches off. An overview of the large instance characteristics is given in Table 3. All three instances are based on the parameters depicted in Table 2. As we consider the described two-way request structure, we have a very large number of requests in these instances, some of which may rarely be used in practical operation.

Table 3. Overview of the large instances' characteristics.

Instance	$|\mathcal{V}|$	$|\mathcal{L}|$	$|\mathcal{P}|$	$|\mathcal{R}|$	Network Length
STR	224	468	51	96,960	14,980 m
CGN	314	602	51	148,100	25,835 m
HAM	170	345	34	31,510	12,680 m

3.2.2. Analysis of Test Instances

The optimal solution to the Fictitious Airport instance with two vehicle types for a value of $\beta = 1$ is shown in Figure 5. PSU nodes and ITU links are colored in red. One PSU is installed at node $g3$. All ITUs are connected to this PSU. The total ITU-length is 1275 m, which means that 25.76 % of the apron road network is equipped with an ITU.

As stated in Table 2, baggage cars have a higher energy intake than buses and at the same time, have lower energy consumption. Consequently, the energy intake for a baggage

car request is always covered if the routing of a baggage care request has large overlaps with those of a bus request when dealing with a particular aircraft parking position; therefore, the question arises under which structural conditions the consideration of different vehicle types is actually necessary in the mathematical model. We analyze four different cases in the Fictitious Airport instance. In Case A, we consider the network as depicted in Figure 5. In Case B, we use the same network structure, but we only consider apron buses as a vehicle type. Hence, no requests start or end at the baggage handling area $bh1$. In Case C and Case D, we exchange the positions of the depot $d1$ and the baggage handling area $bh1$. Thus, the baggage handling area is at the top right corner of the network; however, in Case D we only consider buses as a vehicle type. In all four cases, the energy demand must be met for each considered request ($\beta = 1$).

The results are shown in Table 4. Comparing Case A and B, we find no difference. Hence, it makes no difference in the network in Figure 5 whether we consider the baggage car requests or not. The reason is, that each baggage car request is nearly entirely included in one or more bus requests. If the energy restriction Equation (2) is fulfilled for all $r \in \mathcal{R}_{bus}$, the consideration of baggage cars makes no difference. Since the energy consumption of the buses is larger and the energy intake is smaller than of the baggage cars, the service requests of the buses dominate those of the baggage cars. If we compare the Cases C and D, we find that the baggage cars have a substantial impact on the charging infrastructure in the exchanged network. In Case C, some baggage car requests have no overlap with bus requests, e.g., the request $bh1 - p9 - bh1$. In contrast to the results in Figure 5, a charging infrastructure is built on the right side of the network connecting the nodes $bh1$, $i14$, $i23$ and $i24$. If baggage car requests are not considered (Case D), there is no need for this charging infrastructure resulting in a lower investment. Thus, the structure of the vehicle requests determines the necessity of considering different vehicles types in the model. These results can be transferred to real and more complex airport aprons as follows: If the requests of different vehicles share the majority of the links, only the dominant vehicle type (lower energy intake and higher energy consumption) needs to be considered. If, on the other hand, the percentage of shared links is low, a separate consideration of both vehicle types is necessary.

Table 4. Effects of multiple vehicle types in the Fictitious Airport instance.

Case	ofv	#PSUs	ITU-Length
A	687,500	1	1275
B	687,500	1	1275
C	712,500	3	1125
D	587,500	1	1075

In the DICP-MV, a link cannot be partially equipped with an ITU; however, for the energy consumption of the vehicles, equipping part of the link with an ITU could be sufficient and, and as a result, the total investment may be reduced. To reflect this aspect, we can vary the link lengths for the instances. Thus, the total investment may be reduced if multiple shorter links are considered. We analyze the effect of different link lengths in the Fictitious Airport instance. In the base case of Figure 5, all links have a length of 50 m except for links at terminal nodes and at parking positions, which have a length of 25 m. We analyze five additional structures with reduced link lengths. We add additional nodes to the network to create shorter links. The total lengths of the networks remains unchanged. In the new structures, all links have a length of 25 m, 12.5 m, 5 m, 2.5 m or 1 m.

The results are depicted in Figure 6. We find that decreasing link lengths lead to small investment reductions. If the link lengths are reduced to 1 m, we obtain a reduction of 6.34% in the investment compared to the base case. Simultaneously, the computation time increases from 5 s to 12 h with a remaining optimality gap of 6.3%. Consequently, there is a tradeoff between computation time and investment: considering small link lengths can lead to investment reduction, as well as to a problem with high computation times. A reasonable

link length in the Fictitious Airport instance is a length of 12.5 m, with a computation time of 0.32 h and an investment reduction compared to the base case. (Note: Link lengths are instance-specific. We can not assume that a link length of 12.5 m is beneficial in other instances.) For larger instances, we can assume from these results that the computation time increases strongly for short link lengths; therefore, nodes should initially only be set at intersections of the roads.
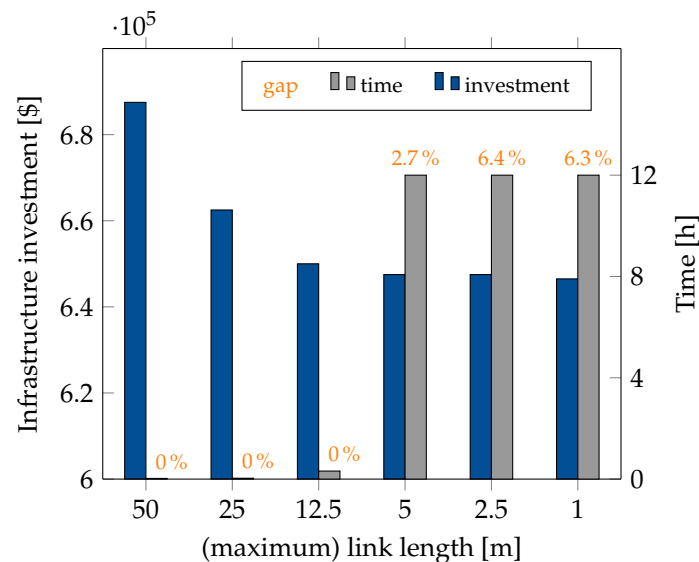
Figure 6. Impact of shorter links in the Fictitious Airport instance (Time limit: 12 h).

The results of the larger instances are depicted in Table 5. The computation time to solve the optimization model using a standard solver (Gurobi) can be substantial, but that is not the relevant topic of this study. As we consider a strategic planning perspective, we set a time limit of seven days as the optimization termination criterion and require the energy demand to be satisfied for each request ($\beta = 1$). Without simplifications, we are unable to solve any of the instances to proven optimality using the standard solver. The remaining optimality gaps are between 7.6% and 13.5%, which indicates that the results are already useful from a practical perspective. Figure 7 shows the solution process in the instances. In the instance HAM, we find a solution close to the best solution found within the first two hours. We do not observe substantial improvements of the Objective Function Value (OFV) within the remaining computation time. For the instances STR and CGN, more time is needed to find a solution; however, as in the case of the instance HAM, a large portion of the computation time is used for very small improvements in the OFV and for proving the optimal solution. This might be due to a large number of symmetric optimal solutions.

To reduce the remaining optimality gap, we have analyze two possible simplifications for the large instances. The results are shown in Table 5. First, we limit the set of links $\mathcal{L}$, that can be equipped with an ITU. Instead of allowing all links to host an ITU, we only use links shared by a large number of requests as possible ITU-candidates. We found a higher investment in all instances with the restricted set $\mathcal{L}$ after the time limit of 168 h. The remaining optimality gap is reduced in all instances, especially in the instances HAM and STR.

Further, we reduce the number of PSU-candidates $v \in \mathcal{P}$. This simplification also reduces the remaining optimality gap. In the instance STR, no reduction in the investment is shown while we obtain a slightly increased investment in the instance HAM and a considerable increase for CGN. A combination of the two simplifications leads to a significant decrease in the remaining optimality gap in all instances. It is even possible to solve all instances HAM to proven optimality within the given time limit; however, we find a tradeoff between the remaining optimality gap and the level of detail: The gap is reduced, but the investment increases (minimally) in all three instances due to the lower level of

detail which is not desirable from an economic point of view. For example, the investment in the instance HAM is 60,000 higher in the simplified case than in the base case.
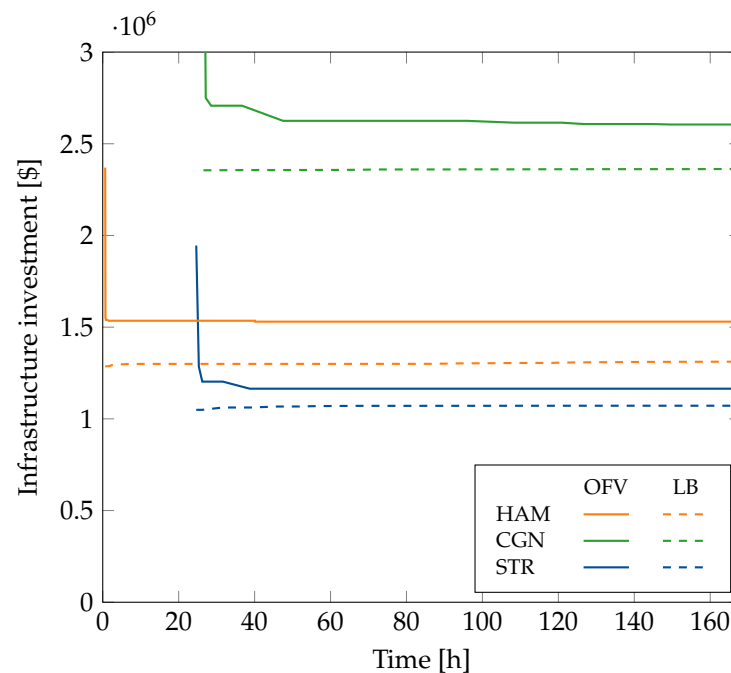

Figure 7. Solution process in the large instances.

Table 5. Analysis of simplifications in the large instances (Time limit: 168 h).

Instance	#PSUs	ITU Candidates	OFV	Difference to Base Case	Time	Gap
HAM						
	34	all	1,530,000	-	168 h	13.5%
	34	specific links	1,570,000	+45,000	168 h	1.8%
	18	all	1,535,000	+5000	168 h	12.7%
	9	all	1,530,000	0	168 h	6.9%
	3	all	1,535,000	+5000	168 h	0.16%
	3	specific links	1,590,000	+60,000	0.62 h	0%
STR						
	51	all	1,159,500	-	168 h	7.6%
	51	specific links	1,295,000	+135,500	168 h	4.4%
	26	all	1,159,500	0	168 h	6.9%
	13	all	1,159,500	0	168 h	6.1%
	4	all	1,159,500	0	168 h	0.47%
	4	specific links	1,295,000	+135,500	62.4 h	0%
CGN						
	51	all	2,602,500	-	168 h	9.2%
	51	specific links	2,620,000	+17,500	168 h	9.1%
	28	all	2,625,000	+22,500	168 h	9.8%
	12	all	2,625,000	+22,500	168 h	8.7%
	6	all	2,625,000	+22,500	168 h	7.2%
	6	specific links	2,605,000	+2500	151.2 h	0%

In all previous calculations, the energy demand had to be met for all possible requests by setting the service level β to a value of one. In the following, we analyze the effects of different service levels in large instances. The results are depicted in Figure 8.

We vary the values for the service level β between 1, which does not allow an energy deficit, and 0.5, which allows a total energy deficit of 50 %. As the allowed energy deficits increase, fewer and fewer ITUs are required to satisfy the energy consumption of the vehicles. Consequently, a decrease in β decreases the total investment for all instances, but may lead to situations where a vehicle cannot pick up as much energy while serving a request as it needs to serve the request, a problem which we study in the subsequent section in detail. It is an important aspect as the right part of Figure 8, which indicates nicely how dramatic the increase in the infrastructure investment is to increase the β-service level of the infrastructure, for instance, from 0.9 to 1.0. In other words, when designing such a charging network, there is a danger of paying a huge price for being overly conservative.
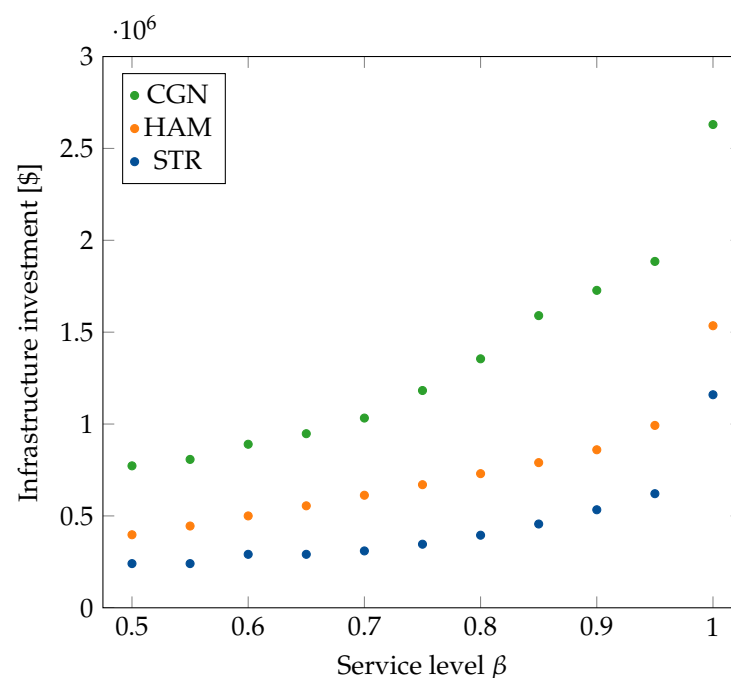
Figure 8. Variation of service level β in large instances (Time limit: 168 h).

Regarding the limitations of the work, it is important to note that in this paper, structural characteristics have been shown on the basis of exemplary instances. For the concrete application of the model, further investigations are undoubtedly necessary, e.g., for the investment and metrics of the individual components of the charging infrastructure. In addition, a larger number of instances would have to be studied to make a general statement about structural effects.

4. Discrete Event Simulation of Typical Airport Apron Procedures

4.1. Objective of the Simulation Study

In Section 3.2.2, we show that reducing the service level β can substantially reduce the infrastructure investment. The question arises how far we can reduce $\beta < 1$ without actually risking a vehicle breakdown due to an empty battery. Note that operating with a charging infrastructure designed for a value of $\beta < 1$ can be possible as in a practical application, any given vehicle typically serves different types of requests over the course of a day. Even if for *some* of the requests it may not be able to pick up the required energy for those particular requests, there is a high probability that while serving a *subsequent* request with a different routing that the vehicle may be able to pick up *more* than the

required energy for that subsequent request, hence eliminating the net energy deficit from the *previous* request.

To study this aspect of the design problem, we develop a simulation model in Python 3.8 that reproduces the service tasks of passenger buses and baggage cars on the airport apron for an entire day. We use the simulation to evaluate the infrastructures proposed by the model presented in Section 3.1 for different service levels β. Moreover, the simulation covers aspects that the model does not consider. One of these aspects is that the battery capacity limits energy intake. With a full battery, the vehicle cannot pick up energy when it travels along an ITU. Moreover, the simulation considers trips where a vehicle travels between two airplane parking positions or two terminal positions. The two-way request structure assumed when designing the charging network for the instances in Table 3 also does not consider these trips. Our simulation model of the vehicle operations on the apron explicitly considers the time-dependent state of charge of the batteries. It hence operates at a greater level of detail than our optimization model to design the charging network in the first place.

4.2. Description of the Simulated Environment

Figure 9 illustrates the relevant operation of the airport apron vehicles. The arrival of an aircraft initiates the arrival process. Passenger buses and baggage vehicles drive to the aircraft when it arrives to pick up the passengers and baggage. Subsequently, the bus travels to the respective gate and the baggage vehicle to the baggage handling area. Note that if the airplane parks at a gate parking position, passengers board the aircraft via the passenger boarding bridge, and therefore, no passenger buses are needed for transfers between the gate and the aircraft. By the time the vehicles have picked up all passengers and baggage from the airplane, the departure process starts. Passengers and baggage are transported from the gate, respectively, the baggage handling area, to the airplane. When all passengers and the luggage arrive at the airplane, the departure process is finished, and the airplane leaves the airplane parking position. Vehicles that are not processing a service request stay at a depot.
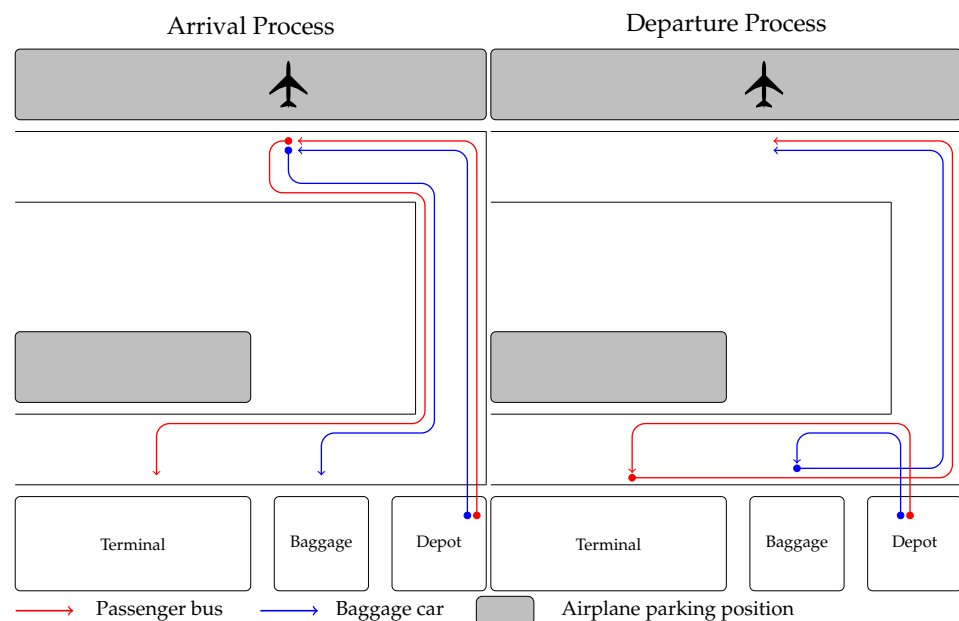
Figure 9. Operation of ground vehicles on an airport apron for the arrival process and departure process.

To represent the state of charge of a vehicles' battery, we assume that while a vehicle drives, it consumes energy and the battery charge level drops. When the vehicle moves along an ITU, the battery charge level increases unless the battery is full. If the vehicle's battery is empty, it breaks down.

A detailed description of the simulation is given in Appendix A.

4.3. Results of the Simulation

4.3.1. Description of the Simulation Parameters

We simulated the operation of passenger buses and baggage vehicles for 24 h for the instances STR, CGN and HAM. During this period, a large number of aircraft arrive. The number of total arrivals is based on the aircraft movements in 2019 for the different airports [41]. Assuming that the flights are equally distributed over the entire year, this results in an arrival rate of 6.8 min for the instance HAM and 7.4 min for the instances CGN and STR. We assume that the inter-arrival time is exponentially distributed over this value.

Passenger buses are assumed to have a passenger capacity of 100 [38]. The actual capacity for luggage vehicles always depends on the number of trailers. We assume that the baggage cars can hold baggage for 100 people. The speed of the vehicles is based on the speed limits [39,40], and is 25 km/h for passenger buses and 20 km/h for luggage vehicles. We assume that loading and unloading the vehicles takes 5 min each.

We distinguish between short-haul, medium-haul and long-haul aircraft. The probability of which aircraft type is involved is based on the distribution of flights at Frankfurt Airport for 2019, with 62% being short-haul flights, 11% medium-haul flights and 27% long-haul flights [42]. An example of a short-haul aircraft is the Boeing 717, which has a capacity of 106 passengers [43]. The Airbus A310 is an example of a medium-haul aircraft and has a capacity of 280 people [44]. The long-haul aircraft A380 has a capacity of 850 people [45]. The passenger numbers of the simulation are based on these real values; however, it must be considered that the flights are not always fully utilized. For this reason, the number of passengers is a random value from a given interval. This interval ranges from 30 to 120 for short-haul aircraft, from 100 to 300 for medium-haul aircraft and from 300 to 800 for long-haul aircraft.

Airplane parking positions, gates and vehicles are selected randomly from those currently available. In addition, the parameters for the energy intake, the energy consumption and the link length are identical to the parameters of the numerical study in Section 3.2.2. Since the energy consumption of the buses is considerably higher than the energy consumption of the luggage vehicles, we assume that their battery has twice the capacity. Every vehicle starts the simulation with a full battery.

4.3.2. Description of the Simulation Results

In the simulation, a vehicle breakdown is due to an empty battery. The battery's state of charge depends on the underlying charging infrastructure resulting from a specific service level β and the size of the battery. The charging infrastructure is a key determinant of the energy supply. If it is not sufficient, the vehicle eventually breaks down due to an empty battery. The size of the battery determines how long a vehicle can function with a deficit between energy intake and energy consumption. If the battery is large enough, it would be possible to drive for an entire day without picking up energy, provided that the vehicle starts the day with a full battery.

For this reason, we simulate the airport apron operations for different service levels and battery capacities. We consider the battery capacities of buses from 10 kWh to 100 kWh with a step size of 10 kWh, and we consider infrastructures of service levels from 0.5 to 1 with a step size of 0.05. For each pair of battery capacity and service level considered, we perform 100 simulation runs to investigate whether vehicles break down due to an empty battery. In the following, we refer to a simulation run where at least one vehicle breaks down as an invalid simulation instance.

Table 6 shows the number of invalid simulation instances out of 100 simulation runs for each pair of the battery capacity and service level. For an increasing service level and an increasing battery capacity, the number of invalid simulation instances decreases. For a service level of 1, no vehicle breaks down in any simulation run. This means that the infrastructures resulting from this service level are very reliable, even if the vehicle's battery

is small. For lower service levels, the vehicle breaks down at low capacities. For example, at a service level of 0.7, no vehicle breaks down from a capacity of 50 kWh for the instances HAM and STR. From these results we can conclude that infrastructures for high service levels β close to 100% tend to be oversized.

Table 6. Invalid simulation instances.

Instance	Capacity in kWh	Service Level β										
		0.5	0.55	0.6	0.65	0.7	0.75	0.8	0.85	0.9	0.95	1
HAM	10	100	100	100	100	100	100	77	62	33	0	0
	20	100	100	100	100	95	34	2	1	0	0	0
	30	100	100	100	100	49	2	0	0	0	0	0
	40	100	100	100	76	1	0	0	0	0	0	0
	50	100	100	94	22	0	0	0	0	0	0	0
	60	100	94	38	0	0	0	0	0	0	0	0
	70	99	66	5	0	0	0	0	0	0	0	0
	80	82	18	0	0	0	0	0	0	0	0	0
	90	27	0	0	0	0	0	0	0	0	0	0
	100	3	0	0	0	0	0	0	0	0	0	0
STR	10	100	100	100	100	100	100	98	44	1	0	0
	20	100	100	100	100	100	99	6	0	0	0	0
	30	100	100	97	100	99	26	0	0	0	0	0
	40	100	100	36	72	24	0	0	0	0	0	0
	50	90	89	0	1	0	0	0	0	0	0	0
	60	22	25	0	0	0	0	0	0	0	0	0
	70	0	0	0	0	0	0	0	0	0	0	0
	80	0	0	0	0	0	0	0	0	0	0	0
	90	0	0	0	0	0	0	0	0	0	0	0
	100	0	0	0	0	0	0	0	0	0	0	0
CGN	10	100	100	100	100	100	100	100	100	100	85	0
	20	100	100	100	100	100	100	100	100	76	0	0
	30	100	100	100	100	100	100	100	94	7	0	0
	40	100	100	100	100	100	100	89	26	0	0	0
	50	100	100	100	100	100	100	54	1	0	0	0
	60	100	100	100	100	100	90	18	0	0	0	0
	70	100	100	100	100	96	59	6	0	0	0	0
	80	100	100	100	99	77	9	0	0	0	0	0
	90	100	100	98	81	33	1	0	0	0	0	0
	100	100	98	80	50	5	0	0	0	0	0	0

However, the specific topology of the apron road network, the routing of the vehicles for the service requests and the structure of the resulting charging network has a major impact on *how far* that service level design parameter β can be reduced. This can nicely be seen for the instance CGN in Table 6. With a service level of 0.7 and a battery capacity of 100 kWh, five simulation runs occur where at least one vehicle breaks down, while for the instance HAM the system still operates smoothly for the same parameter setting.

Figure 10 shows the unused energy supply as a function of the service level for a battery capacity of 100 kWh. The unused energy supply describes the share of energy that the vehicles cannot absorb due to a full battery. In Figure 10 we observe that for all instances with a service level β of 1, approximately 50% of the supplied energy cannot be absorbed by the battery. This supports the conjecture that the resulting infrastructures for a service level of $\beta = 1$ are oversized. With a few exceptions, a decrease in β reduces the unused energy supply.
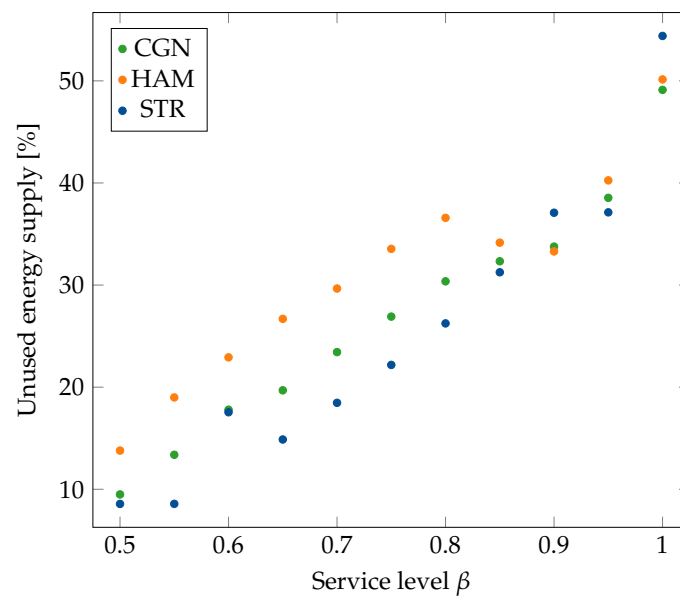
Figure 10. Unused energy supply for different service levels for a bus capacity of 100 kWh.

As the simulation ends after a 24-h period, we cannot make statements on the long-term development of the battery's state of charge. If we assume that the vehicles are in permanent operation exceeding the 24-h period, it is still conceivable that a vehicle eventually breaks down. This can happen if it is *never* charged at its depot, for example during the night, and if the vehicle battery's state of charge is never considered in the dispatching decisions to assign requests for when the possible energy intake exceeds the respective requirement to vehicles with a currently low state of charge. This brings the attention to the *unused energy supply* related to a certain charging infrastructure design.

We suppose the energy provided by the infrastructure to a vehicle is on average higher than the energy consumption. In that case, the vehicle does not break down even in the long run, provided that the battery is large enough to withstand a certain time without energy consumption. Figure 11a,b show the energy balance (energy supply—energy consumption; note that the energy supply includes all the energy provided, regardless of whether the vehicle's battery is fully charged) for different service levels. Figure 11a depicts the energy balance for passenger buses with a battery capacity of 100 kWh and Figure 11a for baggage cars with a battery capacity of 50 kWh. The energy balance is averaged over all vehicles of the considered vehicle type and over 100 simulation runs.

(**a**) Energy balance of passenger buses

(**b**) Energy balance of baggage cars
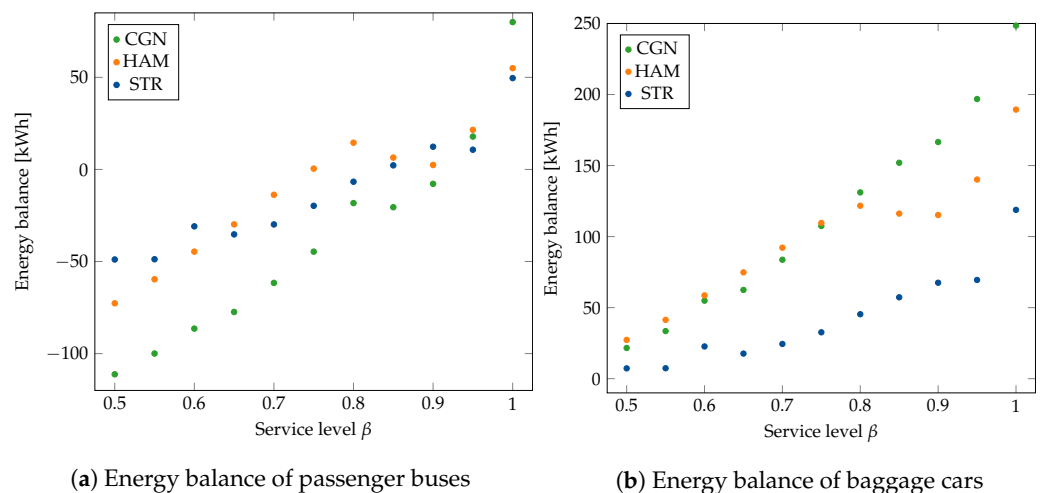
Figure 11. Energy balance for different service levels.

Both figures show that a lower service level leads to a lower energy balance. The decrease in β leads to fewer ITUs in the infrastructure, which reduces the vehicles' energy intake. Figure 11a shows that the energy balance for buses is negative below a certain service level. In the long run, buses in permanent operation break down at these service levels and below. Figure 11b shows that the energy balance for baggage cars is positive for all service levels. Unlike buses, baggage cars frequently serve aircraft parked at the terminal. Compared to the passenger buses, the baggage vehicles travel considerably more in the terminal area. The ITUs are particularly located in the terminal area, an thus, the energy consumption of the baggage vehicles is substantially greater than that of the baggage vehicles. In order to assess whether an infrastructure is suitable for long-term operation, the energy balance of the passenger buses is therefore crucial.

4.3.3. Discussion of the Simulation Results

When implementing a dynamic inductive charging infrastructure on airport aprons, there is a tradeoff between the investment and the reliability of the operation. On the one hand, we can reduce the investment by decreasing the service level. On the other hand, we cannot ensure a reliable long-term operation of the apron vehicles below a certain service level.

If we look at the instance STR, the energy balance for passenger buses is already negative at a service level of 0.8. In Table 6, however, we see that for a battery capacity of the buses of 30 kWh and a service level of 0.8, no vehicle battery depletes in any simulation run. If we were to conduct simulations long enough, vehicles would presumably break down even at these capacities if they were never charged statically at the depot.

Even a positive energy balance does not mean that the battery can be arbitrarily small. For example, the energy balance for passenger buses is positive with a service level of 0.75 for the instance HAM. For capacities up to 30 kWh, however, invalid simulation instances occur. For higher capacities, we can assume that invalid simulation instances do not occur during simulation over a longer time.

The service level with a negative energy balance differs between the instances. For the instance STR, the energy balance is negative below a service level of 0.85 while it is negative for the instance CGN below a service level 0.95. Table 6 has already shown that with the instance CGN invalid simulation instances already occur at much higher service levels. Figure 8 shows that for this instance, decreasing the service level β leads to large investment savings. By reducing β, a considerably smaller charging infrastructure is installed, thus reducing the required investment; however, the vehicles can absorb substantially less energy.

To simulate the operation of electrically powered apron vehicles, simplifying the assumptions that are required that determine the limitations of the results. These simplifying assumptions must be accounted for in the interpretation of the results. For the presented results it is especially important to consider that we assume that all vehicles are moving at a constant speed. As a consequence, only deterministic values for the energy consumption and the energy intake are assumed in the simulation. In reality, however, the driving speed is subject to considerable variations. Furthermore, the energy consumption considered in the simulation is limited only to the distances traveled while serving a request. Other components, such as energy consumption while vehicles are not moving for loading or unloading, are not taken into account.

5. Conclusions

In this paper, we focus on planning a dynamic inductive charging infrastructure for the operation of multiple electrically powered service vehicles on airport aprons. In this context, we derive requirements for the dynamic inductive charging infrastructure to ensure a smooth apron operation. To translate these requirements into a mathematical optimization model, we abstract real-world processes using simplified assumptions. As a result, we introduce the DICP-MV as an MIP.

The numerical study on the DICP-MV uses several fictitious and real-world inspired airport-based test instances of different sizes. We show that the consideration of different vehicle types does have a relevant influence on the resulting charging infrastructure. The impact on the resulting infrastructure is strongly depending on the overlap of the service requests of the different vehicle types. In instances where the different vehicle types travel mostly identical service requests, we find little to no impact on the charging infrastructure; however, in instances where the different vehicle types largely travel on different service requests, we found a substantial impact. In addition, the numerical analysis shows that there is a tradeoff between the investment in charging infrastructure and link length. By reducing the link length, the investment decreases slightly while the computational time increases considerably. For the solution of real-world sized test instances, we observe strongly increasing computation times. A proof of optimality cannot be obtained within seven days of computation time if we use a standard MIP solver; however, the remaining gaps to proven optimality range from around 8% to 15%. One reason for high computation times might be the large number of symmetric optimal solutions. From a practical point of view, however, the solutions found after a few hours of computation time seem to be already useful.

In the simulation, we evaluate the proposed charging infrastructures by the DICP-MV over a 24-h period in an operational setting on the airport apron. We show a tradeoff between the investment in charging infrastructure and the reliability of the operation. By decreasing the service level below a certain threshold, we can decrease the investment, but we cannot ensure a reliable operation of the apron vehicles.

Future research projects could investigate the design of the vehicles and its influence on the inductive charging infrastructure. The air gap between the ITU and the pick-up unit is one aspect of the vehicle design. A smaller air gap leads to a higher efficiency and thus, to a higher energy intake. In addition to the currently investigated problem of designing a dynamic inductive charging infrastructure, the selection among vehicles with different air gaps and prices from potentially different suppliers could be considered. These vehicles have different . A higher price would imply a lower air gap and therefore, a better energy intake. The selection of expensive vehicles with a smaller air gap could lead to savings in the charging infrastructure.

Moreover, the influence of a combination of conductive and dynamic inductive charging could be investigated in future research projects. This would also allow potential downtimes in vehicle depots to be used as potential charging opportunities. In addition, a consideration of the power dimensioning of ITUs and PSUs, as well as additional technological limitations, i.e., maximum length of connected ITUs, are also important future research directions. With respect to the solvability of large instances in particular, the development of problem-specific solution approaches, symmetry-breaking methods and heuristics is intended.

Author Contributions: Conceptualization, J.B.; methodology, J.B.; software, I.N. and N.P.; validation, J.B., I.N., N.P. and S.H.; formal analysis, J.B., I.N. and N.P.; investigation, J.B., I.N. and N.P.; data curation, J.B., I.N. and N.P.; writing—original draft preparation, J.B., I.N. and N.P.; writing—review and editing, S.H.; visualization, J.B., I.N. and N.P.; supervision, S.H.; project administration, S.H.; funding acquisition, S.H. All authors have read and agreed to the published version of the manuscript.

Conflicts of Interest: The authors declare no conflict of interest.

Abbreviations

The following abbreviations are used in this manuscript:

PSU	Power Supply Unit
ITU	Inductive Transmitter Unit
DICP-MV	Dynamic Inductive Charging Problem considering Multiple Vehicle Types
BIP	Binary Integer Program
IP	Integer Program
MIP	Mixed Integer Program
NLP	Nonlinear Program
KAIST	Korea Advanced Institute of Science and Technology
OLEV	On-Line Electric Vehicle
HAM	Airport Hamburg
STR	Airport Stuttgart
CGN	Airport Cologne Bonn
OFV	Objective Function Value
SOC	State of Charge

Appendix A. Description of the Simulation

Appendix A.1. System States

We developed a discrete event-oriented simulation of the vehicles and their batteries' state of charge tailored to this special system. The components of the simulation have states that can change as events occur. Table A1 shows the components of the simulation and their attributes.

The attributes can be either variable or invariable. System states are variable attributes that can, in contrast to invariable attributes, change due to events. The simulation components are vehicles, flights, links, terminal positions and airplane parking positions.

Table A1. Components of the simulation and their attributes.

	System Components		
	Vehicles	**Flight**	**Link** **Terminal Positions,** **Parking Position**
System States	- position - destination - state of charge - availability	- process (arrival/departure)	- availability
Invariable Attributes	- energy consumption per meter - energy intake per meter - person/baggage capacity - battery capacity - speed	- time of arrival - parking position - number of passengers - (arrival/departure) gate	

The system states of the vehicles are the position, destination, state of charge and availability. The position describes the link of the graph on which the vehicle is currently located. The respective destination of the vehicle depends on the service request. Possible destinations are aircraft parking positions, gates, baggage handling areas and depots. We assume that a vehicle always approaches its destination via the shortest path. The availability of a vehicle indicates whether a vehicle is currently at the depot and ready for incoming service requests or whether the vehicle is currently occupied. We assume that vehicles of one vehicle type always travel at the same speed. Hence, speed is an invariant attribute in our simulation. Other invariant attributes are the energy consumption per meter, energy intake per meter, person/baggage capacity and battery capacity. These values are the same for all vehicles of one vehicle type.

As already mentioned, an aircraft is first in an arrival, and then in a departure process. We characterize a flight according to its arrival time, parking position, number of passengers and the assigned arrival or departure gate.

Some positions can only be used by one vehicle or service request at a time. Thus, we consider the availability of the links, aircraft parking position and gates. To neglect interactions when multiple vehicles are traveling on the same link, we assume that only one vehicle can travel on a link at a time. Gates and aircraft parking positions are available for at most one flight at a time. Baggage handling, however, is available for multiple flights.

Appendix A.2. Events

The simulation is composed of five events. An event influences the system states and initiates other events. Table A2 shows these relationships. The arrival of an airplane is the first event of the simulation. The arrival process requires a gate to which buses transport passengers. This gate is occupied until all passengers have arrived. We describe the service trips of the vehicles by three events. The *vehicle starts*, which causes the *vehicle to change its position*, and the *vehicle arrives*.

After an airplane arrives, a sufficient number of available vehicles start their trip from their current position. The number of vehicles is determined by the number of passengers and their capacity. If not enough vehicles are available, the next vehicle that finishes its request is assigned to this flight. All required vehicles are no longer available for other services. The destination of the vehicles is the parking position of the aircraft. We simulate any change in the position of the vehicles. The time a vehicle needs to change its position is determined by the link length and the vehicle's speed. Each time the vehicle's position changes, the battery charge level updates. The energy consumed over the previously traveled link is subtracted from the state of charge, and the energy absorbed over ITUs is added. The charge level cannot exceed the capacity of the battery. Since only one vehicle is allowed on a single link, this event changes the availability of the links. The vehicle changes its position until it reaches its destination.

Table A2. Events of the simulation.

	System Events			
Aircraft Arrives	**Departure Process Starts**	**Vehicle Starts**	**Vehicle Changes Position**	**Vehicle Arrives**
Influenced System States				
parking position/ gate: - availability	gate: - availability flight: - state	vehicle - availability - destination	vehicle - position - state of charge link - availability	vehicle - availability [a] gate - availability [b] parking position - availability [c]
Triggered Events				
- vehicle starts	- vehicle starts	- vehicle changes position	- vehicle changes position - vehicle arrives [e]	- departure process starts [d] - vehicle starts

a. If the destination is the depot. b. In case it is the last bus of this request that brings or picks up passengers to/from this gate. c. In case it is the last vehicle of this request in a departure process that arrives at the aircraft parking position. d. In case it is the last vehicle of this request in an arrival process that arrives at the aircraft parking position. e. In case the new position is the destination.

Arriving at the aircraft in an arrival process, the vehicle picks up passengers or luggage. After a short time, the vehicle continues to the gate or baggage handling area. When the last vehicle has arrived to collect the luggage or passengers, the departure process begins. A gate is assigned for this process and a sufficient number of vehicles drive to the gate or baggage handling area to pick up passengers and baggage. After that, the vehicles travel to the aircraft. A gate is occupied until the last passenger of a flight has been picked up or

brought there. When the last vehicle of the departure process drops off passengers at the aircraft, the aircraft's parking position is free again. If a vehicle has finished a request, it serves a subsequent request or travels to the depot. In the depot, a vehicle is available until it is required for the next request.

References

1. Flughafen München GmbH. Electric Vehicles at the Airport. Available online: https://www.munich-airport.com/electric-vehicles-at-the-airport-5938664 (accessed on 25 January 2022).
2. Dublin Airport. Dublin Airport Becomes Carbon Neutral. Available online: https://www.dublinairport.com/latest-news/2021/01/28/dublin-airport-becomes-carbon-neutral (accessed on 25 January 2022).
3. San Francisco International Airport. *SFO Deploys Its First All-Electric Zero-Emission Buse*s; San Francisco International Airport: San Francisco, CA, USA, 2020.
4. Sheibani, K. Scheduling Aircraft Ground Handling Operations under Uncertainty Using Critical Path Analysis and Monte Carlo Simulation. *Int. J. Bus. Strategy Autom.* **2020**, *1*, 37–45. [CrossRef]
5. Mak, H.Y.; Rong, Y.; Shen, Z.J.M. Infrastructure Planning for Electric Vehicles with Battery Swapping. *Manag. Sci.* **2013**, *59*, 1557–1575. [CrossRef]
6. Jang, Y.J.; Jeong, S.; Ko, Y.D. System optimization of the On-Line Electric Vehicle operating in a closed environment. *Comput. Ind. Eng.* **2015**, *80*, 222–235. [CrossRef]
7. Bundesministerium der Finanzen. AfA-Tabelle für den Wirtschaftszweig "Luftfahrtunternehmen und Flughafenbetriebe". 1994. Available online: https://www.bundesfinanzministerium.de/Content/DE/Standardartikel/Themen/Steuern/Weitere_Steuerthemen/Betriebspruefung/AfA-Tabellen/AfA-Tabelle_Luftfahrtunternehmen-und-Flughafenbetriebe.html (accessed on 26 January 2022).
8. Helber, S.; Broihan, J.; Jang, Y.; Hecker, P.; Feuerle, T. Location Planning for Dynamic Wireless Charging Systems for Electric Airport Passenger Buses. *Energies* **2018**, *11*, 258. [CrossRef]
9. Lukic, S.; Pantic, Z. Cutting the Cord: Static and Dynamic Inductive Wireless Charging of Electric Vehicles. *IEEE Electrif. Mag.* **2013**, *1*, 57–64. [CrossRef]
10. Ahmad, A.; Alam, M.S.; Chabaan, R. A Comprehensive Review of Wireless Charging Technologies for Electric Vehicles. *IEEE Trans. Transp. Electrif.* **2018**, *4*, 38–63. [CrossRef]
11. Moon, S.; Kim, B.C.; Cho, S.Y.; Ahn, C.H.; Moon, G.W. Analysis and Design of a Wireless Power Transfer System With an Intermediate Coil for High Efficiency. *IEEE Trans. Ind. Electron.* **2014**, *61*, 5861–5870. [CrossRef]
12. Panchal, C.; Stegen, S.; Lu, J. Review of static and dynamic wireless electric vehicle charging system. *Eng. Sci. Technol. Int. J.* **2018**, *21*, 922–937. [CrossRef]
13. Throngnumchai, K.; Hanamura, A.; Naruse, Y.; Takeda, K. Design and evaluation of a wireless power transfer system with road embedded transmitter coils for dynamic charging of electric vehicles. In Proceedings of the 2013 World Electric Vehicle Symposium and Exhibition, Barcelona, Spain, 17–20 November 2013; pp. 1–10. [CrossRef]
14. Oak Ridge National Labatory. ORNL Demonstrates 120-Kilowatt Wireless Charging for Vehicles. Available online: https://www.ornl.gov/news/ornl-demonstrates-120-kilowatt-wireless-charging-vehicles (accessed on 25 January 2022).
15. Magment GmbH. Dynamic Wireless Charging. Available online: https://www.magment.de/en-dynamic-wireless-charging (accessed on 18 January 2022).
16. Jang, Y.J.; Suh, E.S.; Kim, J.W. System Architecture and Mathematical Models of Electric Transit Bus System Utilizing Wireless Power Transfer Technology. *IEEE Syst. J.* **2016**, *10*, 495–506. [CrossRef]
17. Jeong, S.; Jang, Y.J.; Kum, D. Economic Analysis of the Dynamic Charging Electric Vehicle. *IEEE Trans. Power Electron.* **2015**, *30*, 6368–6377. [CrossRef]
18. Hwang, I.; Jang, Y.J.; Ko, Y.D.; Lee, M.S. System Optimization for Dynamic Wireless Charging Electric Vehicles Operating in a Multiple-Route Environment. *IEEE Trans. Intell. Transp. Syst.* **2018**, *19*, 1709–1726. [CrossRef]
19. Smart Road Gotland. The World's First Wireless Electric Road Charging an E-Bus and an E-Truck. Available online: https://www.smartroadgotland.com/ (accessed on 25 January 2022).
20. Cision. Successful Start for world's First Wireless Electric Road for Trucks. Available online: https://news.cision.com/electreon-ab/r/successful-start-for-world-s-first-wireless-electric-road-for-trucks,c3062153 (accessed on 14 January 2022).
21. ElectReon. ElectReon Projects: Gotland. Available online: https://www.electreon.com/projects-gotland (accessed on 19 January 2022).
22. ElectReon. ElectReon Projects: Tel Aviv. Available online: https://www.electreon.com/projects-tel-aviv (accessed on 18 January 2022).
23. U.S. Department of Transportation. Surface Movement Guidance and Control System. 1996. Available online: https://rosap.ntl.bts.gov/view/dot/13288 (accessed on 27 January 2022).
24. Schlegel, A. *Bodenabfertigungsprozesse im Luftverkehr: Eine statistische Analyse am Beispiel der Deutschen Lufthansa AG am Flughafen Frankfurt/Main*; Gabler: Wiesbaden, Germany, 2010. [CrossRef]
25. Ashford, N.J.; Stanton, H.P.M.; Moore, C.A.; Coutu, P.; Beasley, J.R. (Eds.) *Airport Operations*, 3rd ed.; McGraw Hill: New York, NY, USA, 2013.

26. Alonso Tabares, D.; Mora-Camino, F. Aircraft ground operations: Steps towards automation. *CEAS Aeronaut. J.* **2019**, *10*, 965–974. [CrossRef]

27. Jang, Y.J. Survey of the operation and system study on wireless charging electric vehicle systems. *Transp. Res. Part C Emerg. Technol.* **2018**, *95*, 844–866. [CrossRef]

28. Yatnalkar, G.; Narman, H. Survey on Wireless Charging and Placement of Stations for Electric Vehicles. In Proceedings of the 2018 IEEE International Symposium on Signal Processing and Information Technology (ISSPIT), Louisville, KY, USA, 6–8 December 2018; pp. 526–531. [CrossRef]

29. Majhi, R.C.; Ranjitkar, P.; Sheng, M.; Covic, G.A.; Wilson, D.J. A systematic review of charging infrastructure location problem for electric vehicles. *Transp. Rev.* **2021**, *41*, 432–455. [CrossRef]

30. Ushijima-Mwesigwa, H.; Khan, Z.; Chowdhury, M.A.; Safro, I. Optimal Placement of wireless charging lanes in road networks. *J. Ind. Manag. Optim.* **2021**, *17*, 1315–1341. [CrossRef]

31. Liu, Z.; Song, Z.; He, Y. Optimal Deployment of Dynamic Wireless Charging Facilities for an Electric Bus System. *Transp. Res. Rec. J. Transp. Res. Board* **2017**, *2647*, 100–108. [CrossRef]

32. Khalaf, A.F.; Jain, K.K.; Noutiyal, A.; Wang, Y. Optimization of Dynamic Wireless Charging in Binghamton University Bus Network: Optimal Locations and Battery Size. In Proceedings of the 7th Annual World Conference of the Society for Industrial and Systems Engineering, Binghamton, NY, USA, 11–12 October 2018.

33. Bi, Z.; Keoleian, G.A.; Ersal, T. Wireless charger deployment for an electric bus network: A multi-objective life cycle optimization. *Appl. Energy* **2018**, *225*, 1090–1101. [CrossRef]

34. Lee, H.; Ji, D.; Cho, D.H. Optimal Design of Wireless Charging Electric Bus System Based on Reinforcement Learning. *Energies* **2019**, *12*, 1229. [CrossRef]

35. Mohamed, A.A.S.; Meintz, A.; Zhu, L. System Design and Optimization of In-Route Wireless Charging Infrastructure for Shared Automated Electric Vehicles. *IEEE Access* **2019**, *7*, 79968–79979. [CrossRef]

36. Iliopoulou, C.; Kepaptsoglou, K. Integrated transit route network design and infrastructure planning for on-line electric vehicles. *Transp. Res. Part D Transp. Environ.* **2019**, *77*, 178–197. [CrossRef]

37. He, J.; Yang, H.; Tang, T.Q.; Huang, H.J. Optimal deployment of wireless charging lanes considering their adverse effect on road capacity. *Transp. Res. Part C Emerg. Technol.* **2020**, *111*, 171–184. [CrossRef]

38. Siemens AG. Electric Bus for Airports: Solution for Sustainable Passenger Transport. Available online: https://assets.new.siemens.com/siemens/assets/api/uuid:52495109232b1176df25668b35daa19243bf8b58/electric-bus-for-airports-en.pdf (accessed on 22 September 2021).

39. Flughafen Hannover-Langenhagen GmbH. Verkehrs- und Zulassungsregeln: Für den Sicherheitsbereich des Flughafengeländes des Flughafens Hannover-Langenhagen. Available online: https://www.hannover-airport.de/fileadmin/downloads/B2B_und_Geschäftskunden/Entgelte_und_AGB/AGB_und_Entgelttabellen/Verkehrs-_und_Zulassungsregeln_für_den_Sicherheitsbereich.pdf (accessed on 26 January 2022).

40. Fraport AG. C2.4 Verkehrs-und Zulassungsregeln. Available online: https://www.fraport.com/de/geschaeftsfelder/service/flughafenausweise/allgemeine-informationen.html (accessed on 25 January 2022).

41. Arbeitsgemeinschaft Deutscher Verkehrsflughäfen. ADV-Monatsstatistik 12/2019. Available online: https://www.adv.aero/service/downloadbibliothek/ (accessed on 25 January 2022).

42. Schultheiß-Münch, M.; Draxler, H.A.; Gerkhausen, C.P.; Wewering, J. *Frankfurt Airport Luftverkehrsstatistik*; Fraport AG: Frankfurt am Main, Germany, 2019.

43. The Boeing Company. 717-200 Technical Characteristics. Available online: https://www.boeing.com/commercial/aeromagazine/aero_19/717_characteristics.pdf (accessed on 17 January 2021).

44. Airbus. A310. Available online: https://www.airbus.com/en/who-we-are/our-history/commercial-aircraft-history/previous-generation-aircraft/a310 (accessed on 23 January 2021).

45. Airbus. A380: Facts and Figures. Available online: https://www.airbus.com/sites/g/files/jlcbta136/files/2021-12/EN-Airbus-A380-Facts-and-Figures-December-2021_0.pdf (accessed on 23 January 2021).